British Journal of Pharmacology

DOI:10.1111/j.1476-5381.2011.01396.x
www.brjpharmacol.org

RESEARCH PAPER

Hydrophobic anions potently and uncompetitively antagonize $GABA_A$ receptor function in the absence of a conventional binding site

Correspondence
Steven Mennerick, Departments of Psychiatry and Anatomy & Neurobiology, Washington University School of Medicine, 660 S. Euclid Avenue, Box 8134, St. Louis, MO 63110, USA.
E-mail: menneris@wustl.edu

Keywords
antagonist; voltage sensor; hippocampal; $GABA_A$ receptors; membrane capacitance

Received
12 January 2011
Revised
18 February 2011
Accepted
17 March 2011

M Chisari[1], K Wu[1], CF Zorumski[1,2] and S Mennerick[1,2]

[1]*Departments of Psychiatry and* [2]*Anatomy & Neurobiology, Washington University School of Medicine, St. Louis, MO, USA*

BACKGROUND AND PURPOSE

A 'lock-and-key' binding site typically accounts for the effect of receptor antagonists. However, sulphated neurosteroids are potent non-competitive antagonists of $GABA_A$ receptors without a clear structure–activity relationship. To gain new insights, we tested two structurally unrelated hydrophobic anions with superficially similar properties to sulphated neurosteroids.

EXPERIMENTAL APPROACH

We used voltage-clamp techniques in *Xenopus* oocytes and hippocampal neurons to characterize dipicrylamine (DPA) and tetraphenylborate (TPB), compounds previously used to probe membrane structure and voltage-gated ion channel function.

KEY RESULTS

Both DPA and TPB potently antagonized $GABA_A$ receptors. DPA exhibited an IC_{50} near 60 nM at half-maximal GABA concentration and antagonism with features indistinguishable from pregnenolone sulphate antagonism, including sensitivity to a point mutation in transmembrane domain 2 of the α1 subunit. Bovine serum albumin, which scavenges free membrane-associated DPA, accelerated both capacitance offset and antagonism washout. Membrane interactions and antagonism were explored using the voltage-dependent movement of DPA between membrane leaflets. Washout of DPA antagonism was strongly voltage-dependent, paralleling DPA membrane loss, although steady-state antagonism lacked voltage dependence. At antagonist concentrations, DPA failed to affect inhibitory post-synaptic current (IPSC) amplitude or decay, but DPA accelerated pharmacologically prolonged IPSCs.

CONCLUSIONS AND IMPLICATIONS

Neurosteroid-like $GABA_A$ receptor antagonism appears to lacks a conventional binding site. These features highlight key roles of membrane interactions in antagonism. Because its membrane mobility can be controlled, DPA may be a useful probe of $GABA_A$ receptors, but its effects on excitability via $GABA_A$ receptors raise caveats for its use in monitoring neuronal activity.

Abbreviations

3α5αP, (3α,5α)-3-hydroxypregnan-20-one; DiO, 3,3′-dihexadecyloxacarbocyanine perchlorate; DPA, dipicrylamine; FRET, Förster resonance energy transfer; P4S, piperidine-4-sulphonic acid; PS, pregnenolone sulphate; TPB, tetraphenylborate

Introduction

Because $GABA_A$ receptors mediate widespread fast neuronal inhibition, they are the target of clinically important drugs and are the object of intense investigation in neuroscience. New tools to probe the mechanisms of receptor gating and function could be important aids experimentally and in some contexts may also be clinically beneficial (Klaassen *et al.*,

2006). Amongst inhibitors, negatively charged sulphated steroids, such as pregnenolone sulphate (PS), uncompetitively inhibit $GABA_A$ receptor-mediated current (Shen *et al.*, 2000; Eisenman *et al.*, 2003). That is, antagonism is dependent upon channel opening and/or desensitization (Pennefather and Quastel, 1992). Although 'uncompetitive' can have multiple meanings when applied to channel blockers (Johnson and Kotermanski, 2006), evidence to date does not support a channel block mechanism for PS and related antagonists (Akk *et al.*, 2001). State-dependent allosteric effects are more likely to explain PS antagonism (Shen *et al.*, 2000; Akk *et al.*, 2001; Eisenman *et al.*, 2003).

Interestingly, several amphiphilic compounds that are structurally unrelated to sulphated steroids may modulate $GABA_A$ receptors by a similar uncompetitive mechanism (Chisari *et al.*, 2010b). Furthermore, PS and other sulphated neurosteroids have non-specific effects on membrane capacitance (Mennerick *et al.*, 2008) and exhibit weak enantioselectivity at $GABA_A$ receptors (Nilsson *et al.*, 1998). These observations might suggest that antagonism is less related to a specific binding site on $GABA_A$ receptors than to local membrane perturbations that alter channel gating (Sogaard *et al.*, 2006). On the other hand, studies of related receptors suggest stronger specificity of actions and the possibility of a specific binding site (Li *et al.*, 2006; Twede *et al.*, 2007).

To explore issues of structural specificity of $GABA_A$ receptor antagonism and to possibly uncover new $GABA_A$ receptor probes with novel properties, we examined hydrophobic anions unrelated to neurosteroids. We focused on dipicrylamine (DPA), which has a number of important properties with applications to studies of membrane structure and excitability (Bruner, 1975; Fernandez *et al.*, 1983; Bradley *et al.*, 2009). After absorbing to the extracellular surface of the plasma membrane, DPA translocates across the membrane leaflets in a voltage-dependent manner (Ketterer *et al.*, 1971; Benz *et al.*, 1976). DPA's ability to absorb certain light wavelengths has also led to new applications as a voltage sensor in Förster resonance energy transfer (FRET) studies (Chanda *et al.*, 2005a,b; Bradley *et al.*, 2009).

Here we report that DPA strongly antagonizes $GABA_A$ receptor function. Like sulphated neurosteroid inhibition, DPA steady-state antagonism is uncompetitive, enhances receptor desensitization, exhibits little steady-state voltage dependence and is dramatically reduced by a mutation in the transmembrane domain 2 residue V256 of the α1 receptor subunit. Positive voltages strongly slowed recovery from antagonism after removal of free aqueous DPA and also slowed washout of membrane-bound DPA. Therefore, we conclude that membrane-associated DPA is important for antagonism. Notably the inhibitory post-synaptic currents (IPSCs) resisted postsynaptic DPA antagonism. However, DPA significantly reduced decay times of pharmacologically prolonged IPSCs, suggesting that the synaptic agonist transient, although representing a high agonist concentration, is normally too brief to promote uncompetitive antagonism by DPA. In summary, our data are consistent with the idea that structurally dissimilar hydrophobic anions share mechanisms of uncompetitive $GABA_A$ receptor antagonism, possibly implicating plasma membrane modifications in their potent antagonism of channel function.

Methods

Hippocampal cultures

All animal care and experimental procedures were consistent with NIH guidelines and approved by the Washington University Animal Studies Committee. Neuronal cultures were prepared from postnatal day 1–3 rat pups anesthetized with isoflurane. Hippocampi were cut into 500 μm-thick slices and digested with 1 $mg \cdot mL^{-1}$ papain in oxygenated Leibovitz L-15 medium (Invitrogen, Gaithersburg, MD). Tissue was dissociated by mechanical trituration in modified Eagle's medium (Invitrogen) containing 5% horse serum, 5% fetal calf serum, 17 mM D-glucose, 400 μM glutamine, 50 $U \cdot mL^{-1}$ penicillin and 50 $\mu g \cdot mL^{-1}$ streptomycin. Cells were plated in modified Eagle's medium at a density of ~650 $cells \cdot mm^{-2}$ as mass cultures (onto 25 mm cover glasses coated with 5 $mg \cdot mL^{-1}$ collagen) or 100 $cells \cdot mm^{-2}$ as 'microisland' cultures (onto 35 mm plastic culture dishes stamped with collagen microdroplets on a layer of 0.15% agarose). Cultures were maintained at 37°C in a humidified incubator with 5%CO_2/95% air. To inhibit glial proliferation, the anti-mitotic cytosine arabinoside (6.7 μM) was added 3–4 days after plating, and half the culture medium was replaced with Neurobasal medium (Invitrogen) containing 500 μM glutamine, 50 $U \cdot mL^{-1}$ penicillin, 50 $\mu g \cdot mL^{-1}$ streptomycin and B27 supplement (Invitrogen) 4–5 days after plating.

Hippocampal electrophysiology

Whole-cell recordings from neuronal cultures were performed 3–12 days following plating using an Axopatch 200B amplifier (Molecular Devices, Sunnyvale, CA). For capacitance measurements, experiments were performed in neurons 1 day after plating. For recordings, cells were transferred to an extracellular solution containing (in mM): 138 NaCl, 4 KCl, 2 $CaCl_2$, 1 $MgCl_2$, 10 glucose, 10 HEPES, 0.001 2,3-dihydroxy-6-nitro-7-sulphonyl-benzo[f]quinoxaline (NBQX) and 0.01 D-2-amino-5-phosphonovalerate (D-APV) at pH 7.25. Patch pipettes were filled with an internal solution containing (in mM): 130 cesium chloride, 4 NaCl, 5 EGTA, 0.5 $CaCl_2$ and 10 HEPES at pH 7.25. When filled with this solution, pipette tip resistance was 3–6 MΩ. Cells were usually clamped to –70 mV or as indicated in figure legends. For autaptic recordings, patch pipettes were filled with an internal solution containing (in mM): 140 KCl, 4 NaCl, 5 EGTA, 0.5 $CaCl_2$ and 10 HEPES at pH 7.25. Electrode tip resistance was 2.5–3 MΩ, and access resistance (8–10 MΩ) was compensated 80–100% for synaptic recordings. For autaptic responses, cells were stimulated with 1.5 ms pulses to 0 mV from –70 mV to evoke transmitter release. Drug applications were made with a multibarrel, gravity-driven local perfusion system. The system provides a laminar local stream for rapid solution exchanges. The common tip was placed 0.5 mm from the centre of the microscope field. Solution exchange times were 120 ± 14 ms (10–90% rise), estimated from junction current rises at the tip of an open patch pipette. Experiments were performed at room temperature.

Imaging

Hippocampal neurons were stained with 5 μM 3,3′-dihexadecyloxacarbocyanine perchlorate (DiO) for 5 min at

37°C, in the external solution described for electrophysiology experiments. Cells were imaged with an epifluorescent microscope (Nikon TE2000, Melville, NY) with a metal halide lamp, a CoolSnap ES2 camera (Photometrics, Tucson, AZ) and a 40× air objective (0.6 NA). DiO fluorescence was detected with a Chroma filter set 41001 (Chroma Technology, Bellows Falls, VT), employing a HQ480/40 nm excitation filter and an HQ535/50 nm emission filter. DPA was applied using a multibarrel, gravity-driven local perfusion system. Experiments were performed at room temperature. Images were acquired and processed with MetaMorph software (Molecular Devices, Downingtown, PA). Changes in DiO fluorescence, upon DPA application and wash out, were determined at two different voltages (as indicated), applied using a patch pipette filled with cesium chloride (as described for electrophysiology experiments). For display, image brightness and contrast were altered equally for the entire series of images using Metamorph to promote clarity of fluorescence visualization. Intrinsic pixel intensity values were not altered by these changes.

Xenopus *oocyte expression*

Stage V–VI oocytes were obtained from sexually mature female *Xenopus* laevis (*Xenopus* One, Northland, MI) subject to 0.1% tricaine (3-aminobenzoic acid ethyl ester) anaesthesia. Capped mRNA coding for rat $GABA_A$ receptor α1, β2 and γ2L subunits were transcribed *in vitro* from linearized pBluescript vectors containing receptor coding regions using the mMessage mMachine Kit (Ambion, Austin, TX). We defolliculated oocytes in collagenase (2 mg·mL^{-1}) dissolved in calcium-free solution (mM: 96 NaCl, 2 KCl, 1 $MgCl_2$ and 5 HEPES at pH 7.4) while shaking for 20 min at 37° C. Less than 24 h after defolliculation, mRNA subunit transcripts were injected in equal parts for a total of 20–40 ng RNA. Oocytes were cultured for 2–4 days at 18°C in ND96 solution (mM: 96 NaCl, 2 KCl, 1.8 $CaCl_2$, 1 $MgCl_2$ and 10 HEPES at pH 7.4) supplemented with pyruvate (5 mM), penicillin (100 i.u.·mL^{-1}), streptomycin (100 μg·mL^{-1}) and gentamycin (50 μg·mL^{-1}). cDNA encoding rat $GABA_A$ receptor subunits were initially provided by A. Tobin (University of California, Los Angeles, CA; α1), P. Malherbe (Hoffman-La Roche, Switzerland; β2) and C. Fraser (National Institute on Alcohol Abuse and Alcoholism, National Institutes of Health, Bethesda, MD; γ2L).

Oocyte electrophysiology

All two-electrode voltage-clamp experiments were performed in ND96 solution on oocytes 2–4 days following RNA injection. Two-electrode voltage clamp experiments were conducted using a Warner OC-725C amplifier (Hamden, CT), an Axon Instruments Digidata 1322A analogue–digital converter (Union City, CA) and an Automate Scientific ValveLink16 perfusion system (Berkeley, CA) to control drug delivery. Intracellular recordings employed glass pipettes filled with 3 M KCl and with an open tip resistance near 1 MΩ. Drug application used a solenoid controlled, gravity-driven multibarrel perfusion system. Cells were voltage-clamped at membrane potentials indicated in figures and text, typically –70 mV. All measurements of current refer to the final value recorded at the end of the 15–30 s drug application unless explicitly noted. In some experiments, we tested expression of the γ2 subunit by verifying lorazepam sensitivity. We also confirmed that there was no notable difference in the antagonistic actions of DPA on oocytes expressing α1β2γ2 subunits versus oocytes injected with only α1β2 subunits.

Data analysis

Data acquisition and analysis were performed primarily using pCLAMP 9 software (Molecular Devices). Extended analysis was done using Microsoft Excel. Graphical figures and curve fitting were conducted with GraphPad Prism (GraphPad Software, La Jolla, CA) or Sigma Plot software (SPSS Science, Chicago, IL). Data are expressed and displayed as mean ± SEM. Statistical significance was determined using a Student's two-tailed *t*-test or two-way, repeated measures ANOVA, as indicated. Curve fitting of dose–response data was performed with the Hill equation [$I = I_{max}\, C^n/(EC_{50}{}^n + C^n)$], where C is the agonist concentration, I_{max} is the maximum current amplitude, EC_{50} is the agonist concentration that yields a 50% response relative to I_{max} and n is the Hill coefficient. For GABA concentration–response curves, responses were normalized to the highest GABA concentration applied to facilitate comparison of shapes and EC_{50} values. Estimation of IC_{50} was achieved with a fit to the same equation with minimum inhibition constrained to 100% of the response to GABA alone and maximum inhibition assumed to be 0 response.

Materials

All compounds were obtained from Sigma (St. Louis, MO) except for DPA and DiO, which were obtained from Biotium (Hayward, CA). Structures of compounds in Figure 8 were created in Marvin 5.3.8 (http://www.chemaxon.com/products/marvin/). Drug target nomenclature follows Alexander *et al.*, (2009).

Results

Effects of DPA and TPB on GABA currents

In hippocampal neurons, we challenged cells with 1 μM GABA, an approximate EC_2 concentration, and with 20 μM GABA, an approximate EC_{80} concentration (Shu *et al.*, 2004), in the absence and presence of 0.5 μM DPA. Figure 1A and B shows that DPA dramatically antagonized GABA-induced currents, especially currents elicited by the higher concentration of agonist. Overall, in six neurons at 1 μM GABA and three neurons at 20 μM GABA, 0.5 μM DPA inhibited steady-state GABA currents to 29.4 ± 0.04% and to 8.2 ± 0.02% of baseline respectively. These results are typical of uncompetitive antagonism and suggest that, like antagonism by PS and picrotoxin, DPA antagonism of $GABA_A$ receptors is at least partly dependent on agonist binding or channel activation (Yoon *et al.*, 1993; Shen *et al.*, 2000; Eisenman *et al.*, 2003).

Hippocampal neurons may express a mixture of receptor subunit combinations with different GABA affinities, which might influence these results. To test DPA's actions on a purer population of $GABA_A$ receptor subunits, we examined α1β2γ2L subunits expressed in *Xenopus* oocytes (Figure 1C). Similar to hippocampal neurons, DPA antagonized GABA responses, especially at high GABA concentrations. Also, in

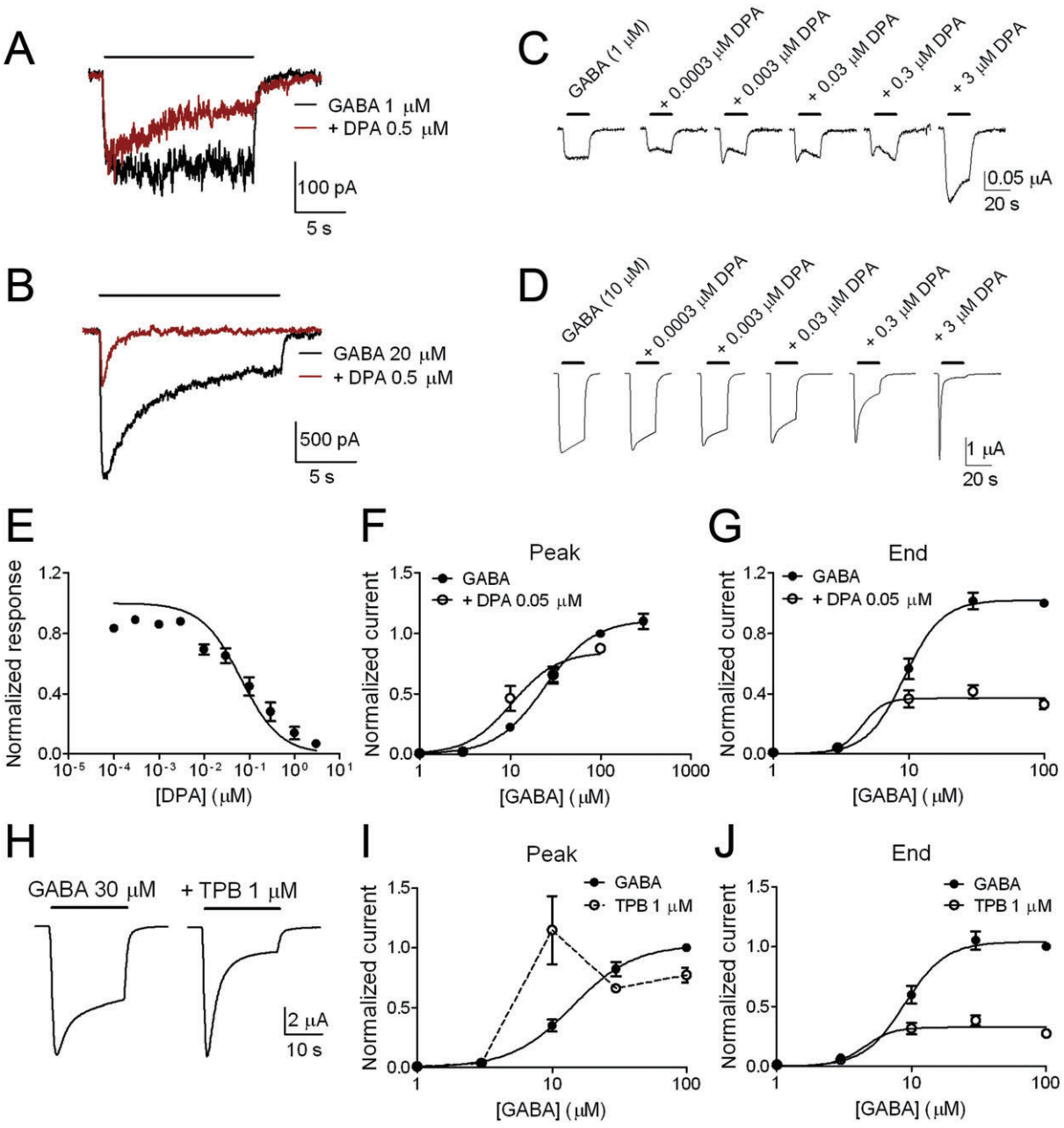

Figure 1

DPA antagonism is dependent on GABA concentration. A. Current response of a hippocampal neuron to a low concentration of GABA (1 μM), then to co-application of GABA plus 0.5 μM DPA. B. Similar protocol on another neuron, except using 20 μM GABA. GABA/DPA co-application resulted in nearly complete inhibition. C. Effects of varied DPA concentrations at 1 μM GABA in an oocyte expressing α1β2γ2L $GABA_A$ receptors. In some batches of oocytes, including this one, there were apparent biphasic effects of DPA, with little overall inhibition at any concentration. D. In the same oocyte, DPA exhibited concentration-dependent inhibition at 10 μM GABA. E. Inhibition curve obtained by measuring the responses at the end of a 20 s co-application of 10 μM GABA and varied DPA concentrations. The solid line is a fit to the Hill equation, assuming a maximum normalized current of 1.0 and a minimum current of 0. Although there appeared to be a component of inhibition that was relatively insensitive to GABA and DPA concentration (evident as weak inhibition at the lowest DPA concentrations), the major component exhibited an IC_{50} of 65 nM. Data points represent the responses of four oocytes. F and G. GABA concentration–response relationships for the peak and final (end) currents during co-application of varied GABA concentrations with a constant DPA concentration (0.05 μM). Antagonism was strongest at the end of the response to the highest GABA concentrations. Solid lines represent fits to the Hill equation. Parameters from the summary fits for GABA alone and in the presence of DPA, respectively, were as follows: for the peak, EC_{50} = 24.2 and 10.5 μM, Hill coefficient = 1.6 and 1.8; for the end, EC_{50} = 9.3 and 4.5 μM, Hill coefficient 3.1 and 5.3. For panels F and G, n = 4 oocytes. H–J. Tetraphenylborate (TPB; 1 μM) inhibition of GABA responses in oocytes. H. Representative responses of 30 μM GABA in the absence and presence of co-applied 1 μM TPB. I and J. GABA concentration–response relationships for peak and end responses in the absence and presence of TPB (n = 3 oocytes). Although TPB was less potent, the pattern of inhibition was strikingly similar to that of DPA.

receptors expressing only α1β2 subunits, the DPA antagonism showed no obvious difference from receptors containing a γ2 subunit (verified by lorazepam sensitivity; data not shown). In oocytes expressing the typical α1β2γ2L subunit combination, we sporadically observed potentiation of GABA responses at the highest concentrations of DPA tested, combined with low GABA concentrations (Figure 1C). This phenomenon was not observed in all batches of oocytes and was not evident in hippocampal neurons. However, mixed potentiation/inhibition is similar to the effects of other amphiphilic compounds (Chisari *et al.*, 2010b). Potentiation was most robust at low agonist concentrations, consistent with the effects of many positive allosteric modulators.

A concentration–response analysis of the effect on DPA on the response to a 20 s, 10 μM GABA application (approximate EC_{50} in oocytes) (Wang *et al.*, 2002), suggested an IC_{50} of 65 nM (Figure 1E). However, in oocytes DPA also exhibited weak antagonism at low GABA concentrations that was relatively independent of DPA concentration (Figure 1C and E). Sensitivity of oocytes to antagonism also appeared to be somewhat lower than that of neurons (compare Figure 1A and C). This might result from subunit differences between oocytes and native cells or from differences in membrane partitioning of DPA (see membrane capacitance studies below) or in differences in GABA EC_{50} values.

We systematically tested the effect of 0.05 μM DPA across a range of GABA concentrations in oocytes (Figure 1F and G). Peak currents were relatively unaffected (Figure 1F). Final current levels elicited by 20 s applications of high GABA concentrations were severely reduced, but steady-state responses to low GABA concentrations were barely affected (Figure 1G). These results indicate that DPA effects on GABA responses are non-competitive with respect to agonist.

As a further test of our hypothesis that structurally diverse hydrophobic anions antagonize $GABA_A$ receptor function, we examined tetraphenylborate (TPB), another membrane probe used in classical biophysical studies (Andersen and Fuchs , 1975; Benz *et al.*, 1976). In four oocytes, TPB antagonized responses to 10 μM GABA with an IC_{50} of near 1 μM for steady-state GABA currents (data not shown); 1 μM TPB added to varying concentrations of GABA yielded a profile of inhibition quite similar to that of DPA (Figure 1H–J), including mixed potentiation/inhibition at some concentration combinations (Figure 1I) and relatively stronger effects on steady-state currents at high GABA concentrations (Figure 1J).

Tests of similarity of actions between DPA and sulphated neurosteroids

Because of DPA's low IC_{50}, we focused on it in subsequent experiments. We first explored whether DPA antagonism is mechanistically similar to those of a better characterized hydrophobic anion, the sulphated neurosteroid PS. PS exhibits a number of signature characteristics that we tested in Figures 2 and 3. These include dependence on channel activation, weak antagonism against high-affinity, partial $GABA_A$ receptor agonists and sensitivity to a point mutation that leaves modulation by other uncompetitive antagonists intact (Shen *et al.*, 2000; Eisenman *et al.*, 2003).

DPA antagonism of both hippocampal and oocyte GABA responses featured a strong increase in apparent desensitization (Figure 1). This profile could represent uncompetitive DPA antagonism (e.g. channel block or conformation-dependent antagonism), or the profile could simply suggest that DPA binds its site more slowly than GABA binds to its site. In oocytes, slow binding is particularly difficult to distinguish from slow kinetics because the large surface area of oocytes prevents rapid solution exchanges, and binding can be artificially slowed by this technical consideration. To distinguish slow DPA binding from uncompetitive antagonism, we performed experiments on young neurons (3–5 days *in vitro*) with limited dendritic arbors, thus facilitating rapid, complete solution exchanges. We compared the effect of our standard simultaneous GABA/DPA co-application protocol with pre-application of DPA for 15 s prior to co-application with GABA (Figure 2A and B). Traces for this experiment are shown in Figure 2A and B. The same protocol was applied in older neuronal cultures with similar results (7–8 days *in vitro*;

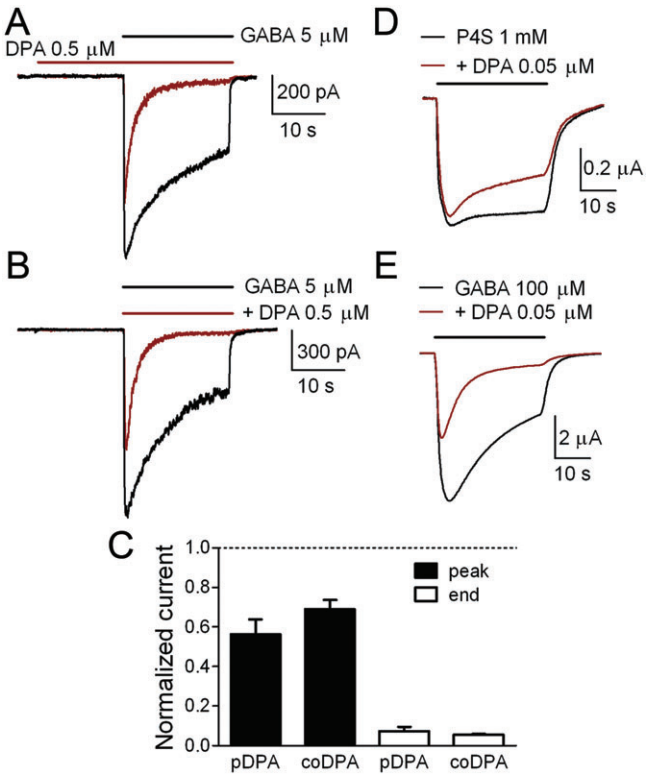

Figure 2

Dependence of DPA antagonism on channel activation. A. Pre-application protocol in a hippocampal neuron to allow any slow binding of DPA to occur before channel activation by GABA. B. Corresponding protocol in another cell in which DPA and GABA were co-applied. Note the similarity of response profiles in the two protocols, suggesting that uncompetitive antagonism is the primary cause of the apparent desensitization profile. C. Summary of the effect of DPA in the pre-application (pDPA, $n = 7$) and co-application (coDPA, $n = 5$) protocols. The effect of DPA on the peak GABA current and the current at the end of GABA/DPA co-application is shown. D. Oocyte response to a saturating concentration of the high-affinity partial agonist P4S in the presence and absence of co-applied DPA. E. Response of the same oocyte to 100 μM GABA in the absence and presence of DPA.

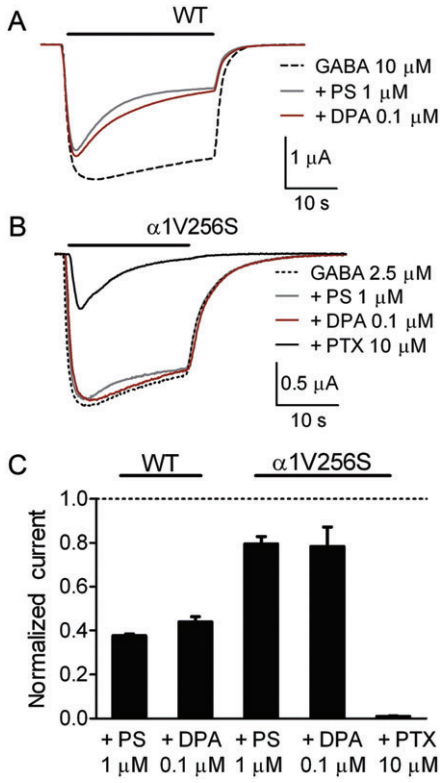

Figure 3

A point mutation reveals similarity of PS and DPA mechanisms. A. Comparison of the actions of 0.1 μM DPA and 1 μM pregnenolone sulphate (PS) on the response to 10 μM GABA. Note that although the profile of inhibition is the same, the IC_{50} of aqueous DPA is approximately 10-fold higher than that of PS. B. In the α1 point mutation V256S, both DPA and PS inhibition are severely attenuated. GABA concentration was adjusted to account for the GABA EC_{50} shift induced by the mutation (Wang *et al.*, 2002; Chisari *et al.*, 2010b). Despite near loss in sensitivity to both sulphated steroid and DPA antagonism, another non-competitive antagonist, picrotoxin (PTX), still strongly inhibited α1V256S responses. C. Left bars: Summary of inhibition of the current at the end of a 30 s application of 10 μM GABA and the two antagonists. $n = 4$ oocytes expressing wild-type receptor subunits. Right bars: Summary of the effects of the three antagonists on α1V256S receptor currents, $n = 12$ oocytes.

data not shown), suggesting that there are no appreciable developmental changes in DPA sensitivity of neuronal GABA currents. Pre-application only slightly reduced GABA peak responses below those achieved with simultaneous GABA/DPA co-application (Figure 2A and B). Thus, pre-equilibration of DPA with receptors to account for any slow binding did not change the profile of responses, and we conclude that agonist binding and/or gating is important for antagonism by DPA.

The more pronounced effect of DPA at higher GABA concentrations (Figure 1) could arise from more effective DPA actions on receptors that are liganded by agonist (but not necessarily opened), or DPA actions might be facilitated by protein conformations downstream of ligand binding (e.g. channel activation or subsequent desensitization) (Shen *et al.*, 2000; Eisenman *et al.*, 2003). To determine whether agonist binding or channel activation/desensitization was more important for the apparent activation dependence of antagonism, we used the partial agonist piperidine-4-sulphonic acid (P4S, 1 mM) (Ebert *et al.*, 1994). P4S binds the $GABA_A$ receptor with high affinity but gates the channel with low efficacy (Ebert *et al.*, 1994). Therefore, when used at a high concentration, P4S binds to all receptors, but relatively few channels are open. The maximum response of P4S relative to GABA is 10–30% (Ebert *et al.*, 1994; Eisenman *et al.*, 2003). If agonist binding is important for antagonism, at high P4S concentration, we would expect DPA (0.05 μM) antagonism to be similar to that observed with a high concentration of the full agonist GABA. On the other hand, if channel conformations downstream of binding are relevant, we would expect weak DPA antagonism. DPA antagonism was clearly weaker against 1 mM P4S compared with 100 μM GABA (Figure 2D and E). In five oocytes tested, inhibition by 0.05 μM DPA was 25 ± 0.02% for 1 mM P4S and 80 ± 0.01% for 100 μM GABA ($P < 0.0001$). The results suggest that channel conformations downstream of ligand binding are most relevant to effective DPA antagonism, although we cannot completely exclude the possibility that ligand-bound, closed conformations might differ for GABA and P4S.

Both picrotoxin and sulphated neurosteroids exhibit features of uncompetitive antagonism explored in Figures 1 and 2. However, a point mutation on the cytoplasmic side of transmembrane domain 2 in the α1 subunit strongly distinguishes the actions of PS from those of picrotoxin (Akk *et al.*, 2001; Eisenman *et al.*, 2003). A valine to serine substitution at position 256 renders receptors nearly insensitive to sulphated steroid antagonism but leaves the receptors strongly sensitive to picrotoxin. To help determine whether DPA actions are more similar to sulphated neurosteroid mechanisms or to picrotoxin mechanisms, we examined the effect of DPA on the recptors containing the α1V256S mutation (Figure 3). For this experiment, we adjusted the GABA concentration to account for the leftward shift in the GABA concentration–response relationship induced by the mutation (Wang *et al.*, 2002; Chisari *et al.*, 2010b). Figure 3B shows that the α1V256S receptors were almost totally resistant to both PS and to DPA antagonism, while retaining sensitivity to picrotoxin. Therefore, we conclude that the mechanism of DPA antagonism bears strong similarity to that of PS but can be distinguished from mechanisms of picrotoxin antagonism.

The role of membrane interactions in receptor antagonism

We predicted that DPA would be a $GABA_A$ receptor antagonist partly because both sulphated neurosteroids (known $GABA_A$ receptor antagonists) and DPA increase membrane capacitance. We were interested in testing the idea that membrane interactions participate in receptor antagonism. First, we explored the slow kinetics of DPA washout. A difference between DPA antagonism and that of PS was the extremely slow washout of DPA effects. This might result from the strong membrane retention of DPA, although it is also possible that the slow removal represents a high binding affinity (slow dissociation) of DPA from a receptor binding site. We used membrane capacitance changes induced by DPA (Ketterer *et al.*, 1971; Bruner, 1975; Benz and Läuger, 1977) to monitor the rate of membrane departitioning. Indeed, mem-

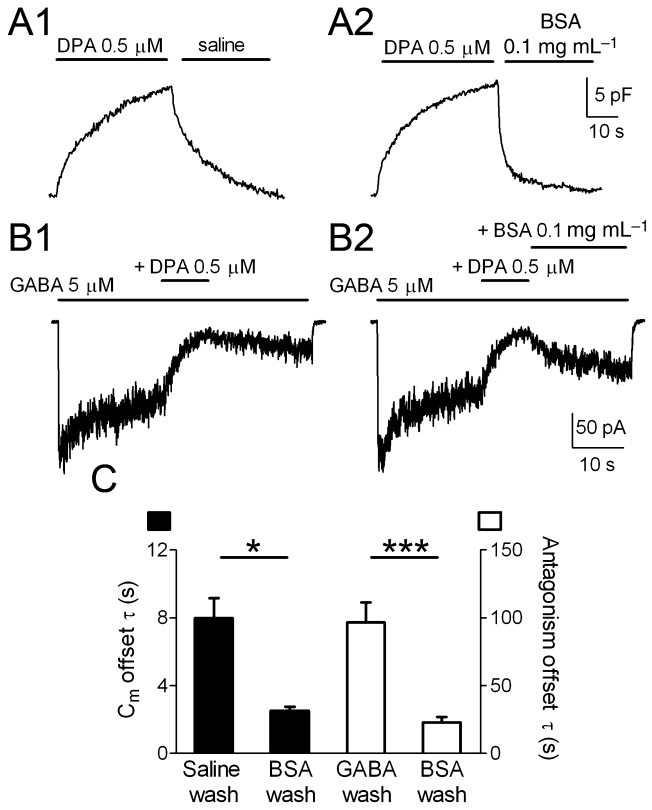

Figure 4

BSA scavenging suggests that DPA partitioning into the plasma membrane is important for antagonism. A1 and A2. Demonstration, using membrane capacitance as a marker of DPA membrane presence, that wash with BSA accelerates DPA departitioning from the plasma membrane. Capacitance was monitored with brief test voltage pulses from a holding potential of –70 mV. B1 and B2. Similar experiment examining the effect of BSA on slow recovery from DPA antagonism on GABA response. BSA significantly accelerates the return of the GABA current following DPA removal. C. Summary of the time constants of washout of DPA-induced capacitance increases and washout of DPA-induced antagonism. Capacitance: $n = 4$ neurons, $^*P < 0.05$, paired *t*-test. Antagonism: $n = 10$ neurons, $^{***}P < 0.0001$, paired *t*-test.

brane departitioning was also slow following removal of aqueous DPA (Figure 4A1). We tried two scavengers of hydrophobic compounds to accelerate the return of membrane capacitance after removal of free aqueous DPA. Cyclodextrins effectively sequester neurosteroids, including PS, and accelerate membrane departitioning (Shu *et al.*, 2007). However, with assays previously applied to neurosteroids (Shu *et al.*, 2007), we found that γ-cyclodextrin failed to complex with DPA (data not shown). This is consistent with the structural dissimilarity of DPA and PS. In contrast, bovine serum albumin (BSA) was a more effective molecular scavenger; BSA significantly accelerated DPA membrane removal (Figure 4A2 and C). If slow washout of antagonism also results from slow removal from the membrane, BSA should also accelerate washout of $GABA_A$ receptor antagonism. On the other hand, if tight receptor binding primarily accounts for the slow kinetics of DPA, BSA should not affect antagonism washout kinetics, since BSA should not alter the dissociation rate constant for bound DPA. Figure 4B and C shows that BSA accelerated the washout of DPA effects on $GABA_A$ receptors, suggesting that membrane interactions are likely to be rate limiting in $GABA_A$ receptor modulation by DPA. Although the recovery of GABA current was slower than the washout of capacitance increases (Figure 4), this could reflect the influence of channel conformational changes (recovery from desensitization following DPA unbinding) to the current recovery, and/or it could reflect the contribution of very small quantities of DPA in the membrane to antagonism.

We next exploited the known voltage dependence of DPA movement in the membrane to explore a role for membrane-associated DPA on $GABA_A$ receptor function (Figure 5). At –70 mV in oocytes, 0.1 μM DPA increased membrane capacitance from a baseline value of 164 ± 4 to 176 ± 6 nF in the presence of DPA (7.1 ± 0.4% increase). A full Boltzmann analysis of charge movement elicited by DPA suggested a $V_{1/2}$ of –59 mV in naïve, uninjected oocytes (Figure 5A and C), very similar to that reported previously (Chanda *et al.*, 2005a). Neurons also exhibited voltage-dependent DPA capacitive charge movement, but at –70 mV, the percentage increase of capacitance at 0.5 μM was much larger than that in oocytes (54.3 ± 5.1%), and the $V_{1/2}$ for DPA-induced charge movement was significantly depolarized relative to oocytes (+13 mV; Figure 5B and C). We observed no significant difference in the $V_{1/2}$ of oocytes expressing $GABA_A$ receptors versus naïve oocytes (Figure 5C). Thus, the presence of $GABA_A$ receptors in the membrane does not explain the difference between the two cell types. The different $V_{1/2}$ in oocytes versus neurons is more likely to arise from asymmetries in plasma membrane composition, which are known to interact with DPA-mediated charge movements (Benz and Läuger, 1977). The voltage dependence of DPA-induced capacitive charge movement contrasts with the behaviour of PS-induced capacitance increases, which exhibit almost no voltage dependence (Mennerick *et al.*, 2008).

For PS, the lack of voltage dependence in capacitive charge movement correlates with weak or no voltage dependence in $GABA_A$ receptor antagonism (Akk *et al.*, 2001; Eisenman *et al.*, 2003). If capacitance increases and $GABA_A$ receptor antagonism are related, the voltage dependence of DPA-induced charge movements predicts that antagonism might exhibit similar voltage dependence and might vary according to the cell type-dependent differences shown in Figure 5A–C. Surprisingly, steady-state $GABA_A$ receptor antagonism was not detectably voltage-dependent in either hippocampal neurons or in oocytes (Figure 5D–F). Furthermore, antagonism was not voltage-dependent at either low or high concentrations of the antagonist (Figure 5F).

This result may suggest that the interaction of DPA with the plasma membrane, as monitored by voltage-dependent charge movement, is not important for DPA antagonism of $GABA_A$ receptors. Alternatively, perhaps $GABA_A$ receptor antagonism is supported by presence of DPA in either membrane leaflet. This latter interpretation was supported by voltage-dependent kinetics of DPA actions in neurons (Figure 6). Offset of DPA antagonism was severely retarded at +40 mV relative to offset/washout at –70 mV (Figure 6A and B). This voltage difference could be consistent with the idea that at +40 mV, more DPA is trapped in the inner membrane

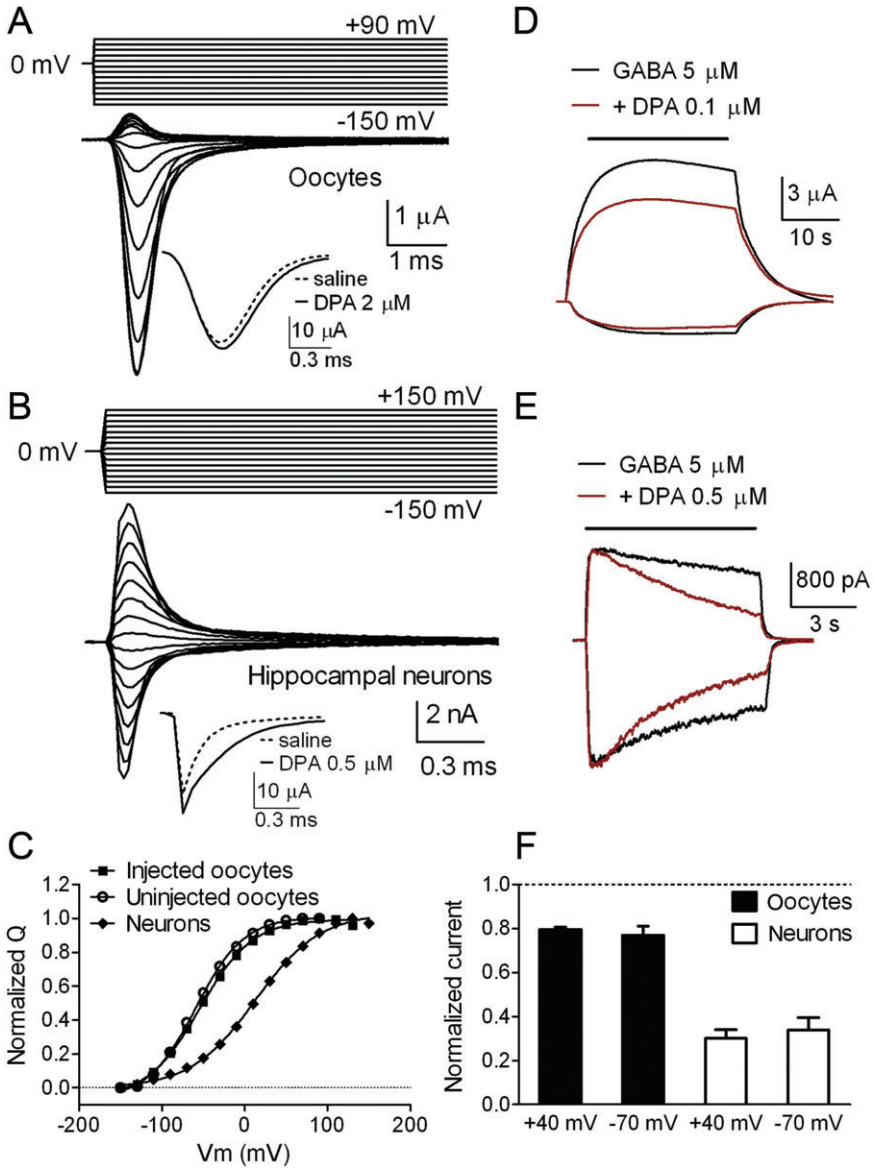

Figure 5

Voltage dependence of DPA interactions with oocyte and neuron plasma membranes, and steady-state voltage dependence of antagonism. A. Voltage dependence of DPA-induced charge movements in a naïve oocyte (not injected with $GABA_A$ receptor cRNA). The DPA-induced charge movements were obtained using a voltage pulse protocol from a holding potential of 0 mV to potentials ranging from –150 to +90 mV (top traces). Current responses in the absence of DPA (example of response to pulse to –90 mV shown in inset) were subtracted from responses in the presence of DPA (also shown in inset) to yield the traces shown in the main panel. B. A similar protocol applied to a hippocampal neuron at 2 days *in vitro*. Note that DPA-induced charge movements exhibit a markedly different voltage dependence than in oocytes. C. Summary plot of voltage dependent charge movements in oocytes injected with $GABA_A$ receptor RNA ($n = 4$), uninjected oocytes ($n = 4$) and in hippocampal neurons ($n = 8$). Error bars for normalized charge movements are smaller than the symbols in all cases. Solid lines are fits to the Boltzmann equation of the form $1 / [1 + \exp(V_{1/2} - V) / S]$. $V_{1/2}$ is the half voltage for maximum charge, V is the test potential and S is a slope factor equivalent to RT/zF. $V_{1/2}$ for oocytes was –54 and –59 mV for injected and uninjected oocytes, respectively, and was +13 mV for neurons. Slope factor was 32, 29 and 39 for the respective groups. At 25°C, the apparent valence, z, was estimated to be –0.81, –0.90 and –0.67 respectively. D. Example of response of an oocyte to co-applied GABA and DPA at –70 mV (inward currents) and +40 mV (outward currents). E. Similar protocol from a hippocampal neuron. F. Left bars: Summary of four oocyte responses at –70 and +40 mV in the protocol depicted in D. Right bars: Summary of inhibition in eight neurons at the two potentials depicted in E. Despite probing strong and weak DPA inhibition with fivefold different DPA concentrations, we found no evidence for voltage-dependent antagonism at either DPA concentration or cell type.

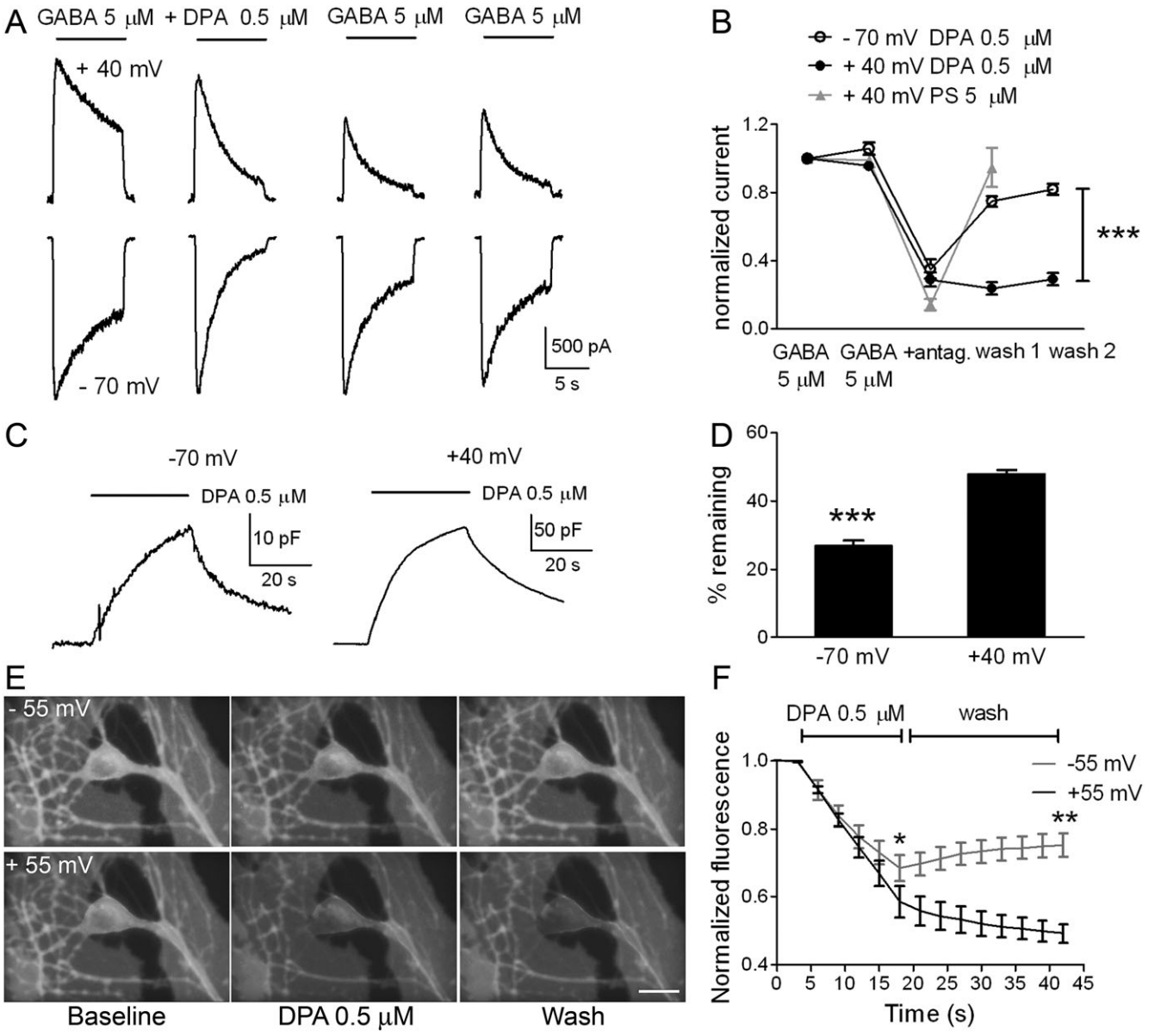

Figure 6

Slow recovery from antagonism at +40 mV. A. Responses at −70 and at +40 mV in a hippocampal neuron to the sequence of GABA and GABA/DPA applications are shown. Applications were separated by a 20 s interval of saline wash. Notice that recovery by the second re-application of GABA alone was more complete at −70 mV than at +40 mV. B. Summary of normalized responses from GABA applications in the sequence shown in A. Before antagonist (antag.) application, stable GABA responses were established (first two data points). End currents have been normalized to the end current in the initial GABA-alone response. $n = 8$ neurons represented in the summary, $^{***}P < 0.0001$ for both GABA washes. The same experimental protocol was used to test PS inhibition and recovery at +40 mV (in gray, $n = 6$). C. Time course of capacitance changes at −70 mV and at +40 mV were tracked as an indication of membrane retention. Membrane capacitance was monitored by brief 20 mV membrane depolarizations from the indicated potential. The smaller apparent change in capacitance at −70 mV arises from the voltage dependence of charge movement shown in Figure 5. Traces are shown with different vertical calibration bars to highlight the washout time course; note the more complete washout relative to the peak capacitance increase at −70 mV. D. Summary of the difference in retention of DPA effects after a 30 s washout at each potential. $n = 6$ neurons, $^{***}P < 0.0001$. E. Retention of DPA at a positive membrane potential monitored with FRET-based fluorescence quenching. For this experiment, we chose membrane potentials within the nearly linear range of expected distribution of DPA in the membrane leaflets (Figure 5C), −55 and +55 mV. The images are of a field containing a voltage-clamped hippocampal neuron at the indicated membrane potentials. The FRET donor DiO was preloaded in the culture dish for 5 min at 37°C. DPA was perfused onto the cell after a whole-cell recording was established. A decrease in DiO fluorescence, at least partly resulting from FRET interaction between DiO and DPA, was observed at both potentials. However, fluorescence was more successfully recovered at the negative potential than at the positive potential during the 24 s wash time. Bar, 10 μm. F. Summary of DiO fluorescence during the indicated periods from three voltage-clamped neurons subjected to the protocol. Some fluorescence loss in this protocol may have resulted from DiO bleaching and/or DiO loss from the membrane during the protocol. However, the contributions should be similar at the two potentials. $^{*}P < 0.05$, $^{**}P < 0.01$.

leaflet, where it is resistant to loss by membrane departitioning, but from where it can still inhibit $GABA_A$ receptor currents. Voltage dependence of washout did not extend to PS antagonism ($n = 6$, Figure 6B), suggesting that the voltage dependence did not arise from basal $GABA_A$ receptor gating differences at the two potentials (Weiss, 1988; Pytel *et al.*, 2006).

To test whether membrane-bound DPA is indeed more resistant to washout at positive membrane potentials, we examined washout of membrane capacitance at negative and positive potentials (Figure 6C and D), using brief voltage pulses from the indicated potential to measure capacitance. Consistent with the observations regarding offset of DPA antagonism, capacitance increases were significantly more resistant to wash at +40 mV than at –70 mV (Figure 6C and D).

We also exploited the ability of DPA to act as a FRET acceptor when paired with the fluorescent inner leaflet membrane probe DiO (Bradley *et al.*, 2009) to evaluate the voltage dependence of DPA's membrane washout. Figure 6E shows DiO fluorescence images from a representative field. In the presence of pre-loaded DiO, DPA induced a fluorescence decrease through FRET interaction at both negative and positive membrane potentials. As expected from the average proximity between DPA and DiO at the two potentials, FRET-induced quenching was stronger at the positive membrane potential (Bradley *et al.*, 2009). On washing, DiO fluorescence returned more rapidly at –55 mV compared with +55 mV (Figure 6E and F). Taken together, the capacitance and imaging results of Figure 6C–F are consistent with the idea that DPA's interactions with the plasma membrane are important for $GABA_A$ receptor antagonism. Possible models reconciling the lack of steady-state voltage dependence of antagonism with the voltage dependence of antagonism washout are considered in the Discussion.

Effects of DPA on synaptic transmission

How do the state-dependent antagonist properties of DPA and its membrane partitioning influence presynaptic and postsynaptic function? To evaluate this, we used autaptic synapses made by solitary hippocampal neurons grown in culture (Bekkers and Stevens, 1991; Mennerick *et al.*, 1995). Evoked synaptic responses were elicited by brief depolarization, which triggers a breakaway action potential in the distal axon of the voltage-clamped neuron. Evoked IPSCs were monitored at a membrane potential of –70 mV with the chloride reversal potential set to 0 mV. The time course and amplitude of IPSCs were not affected by concentrations of DPA that strongly antagonized responses to exogenous GABA in hippocampal neurons. Figure 7A shows a relative lack of effect of 1 μM DPA on baseline IPSCs, except for a small shift in the time of peak IPSC. PS (5 μM), which we estimate to have similar effects on steady-state GABA responses as 0.5 μM DPA (e.g. Figure 3A), also had little effect on peak IPSCs (7.3 ± 0.1% decrease in 6 neurons) but significantly accelerated the IPSC decay (Figures 7B; 42.0 ± 0.1% decrease in the weighted time constant, τ_w). At a higher DPA concentration (2 μM, $n = 3$ neurons), the IPSC was reduced in an all-or-none manner (Figure 7C) and was slowly recoverable (Figure 7C). We attribute the shifted time of peak IPSC and all-or-none loss of IPSCs to the increase in cell capacitance by DPA (Chanda *et al.*, 2005b), which probably slows axonal action potential conduction at low DPA concentrations. At high concentrations, there is complete failure of action potential initiation (Figure 7C inset) and/or propagation. Together, the relative refractoriness of synaptic $GABA_A$ receptors to DPA antagonism suggests that DPA's onset kinetics may be so slow that DPA fails to affect postsynaptic receptors, opened only briefly by the synaptic GABA transient, albeit with high probability at near mM agonist concentration (Maconochie *et al.*, 1994).

If channels during an IPSC are not sufficiently activated during the brief synaptic GABA transient for the DPA antagonism to influence IPSCs, then by artificially prolonging IPSCs, we might unmask a postsynaptic DPA effect. Experiments with three different classes of positive $GABA_A$ receptor modulators to prolong IPSCs supported this hypothesis (Figure 7D–G). Figure 7D shows that 0.5 μM DPA was transformed from inert to active in the presence of 50 nM of the positive $GABA_A$ receptor modulator (3α,5α)-3-hydroxypregnan-20-one (3α5αP, or allopregnanolone). 3α5αP alone prolonged the IPSC decay by approximately threefold (Figure 7E), and there was a nearly complete reversal of the decay time course in the combined presence of DPA and 3α5αP (Figure 7D and E). This inhibition did not result from direct antagonism between 3α5αP and DPA because pentobarbital, another class of positive modulator, functionally interacted with DPA in a similar manner (Figure 7F). Furthermore, PS also greatly accelerated the artificially prolonged IPSCs; weighted decay time constants were 421 ± 1% of control in the presence of 50 nM 3α5αP and were partially reversed (146 ± 0.5% of control) by the co-application of 5 μM PS ($n = 3$).

One possible explanation for the effects of DPA in the presence of 3α5αP and pentobarbital is that GABA spills onto high-affinity, DPA-sensitive extrasynaptic receptors containing δ subunits during the decay phase of the IPSCs, and these high-affinity subunits are selectively blocked by DPA. To test this hypothesis, we used the benzodiazepine lorazepam, a modulator whose potentiation of $GABA_A$ receptors requires the presence of a γ subunit. Thus, any non-γ containing extrasynaptic receptors should not be affected by this positive modulator. In the presence of lorazepam, we again observed a similar pattern of interaction between positive and negative modulators (Figure 7G). We conclude that DPA can be rendered an effective synaptic antagonist during artificial IPSC prolongation.

To test for effects on other ion channels involved in synaptic transmission, we also examined the effect of DPA on AMPA receptor-mediated autaptic excitatory postsynaptic currents (EPSCs). In five cells, 0.5 μM DPA did not significantly alter the peak or decay of EPSCs (Figure 7H and I). This validates the conclusion that up to 0.5 μM, DPA does not directly or indirectly affect the ion channels responsible for action potential waveform, action potential propagation, Ca^{2+} influx or postsynaptic AMPA receptor function. Therefore, under some circumstances, DPA's constellation of properties may make it a useful tool for exploring GABA synaptic function.

Discussion and conclusions

Based on the suggestion that negative modulation of $GABA_A$ receptors may involve general structural attributes (hydropho-

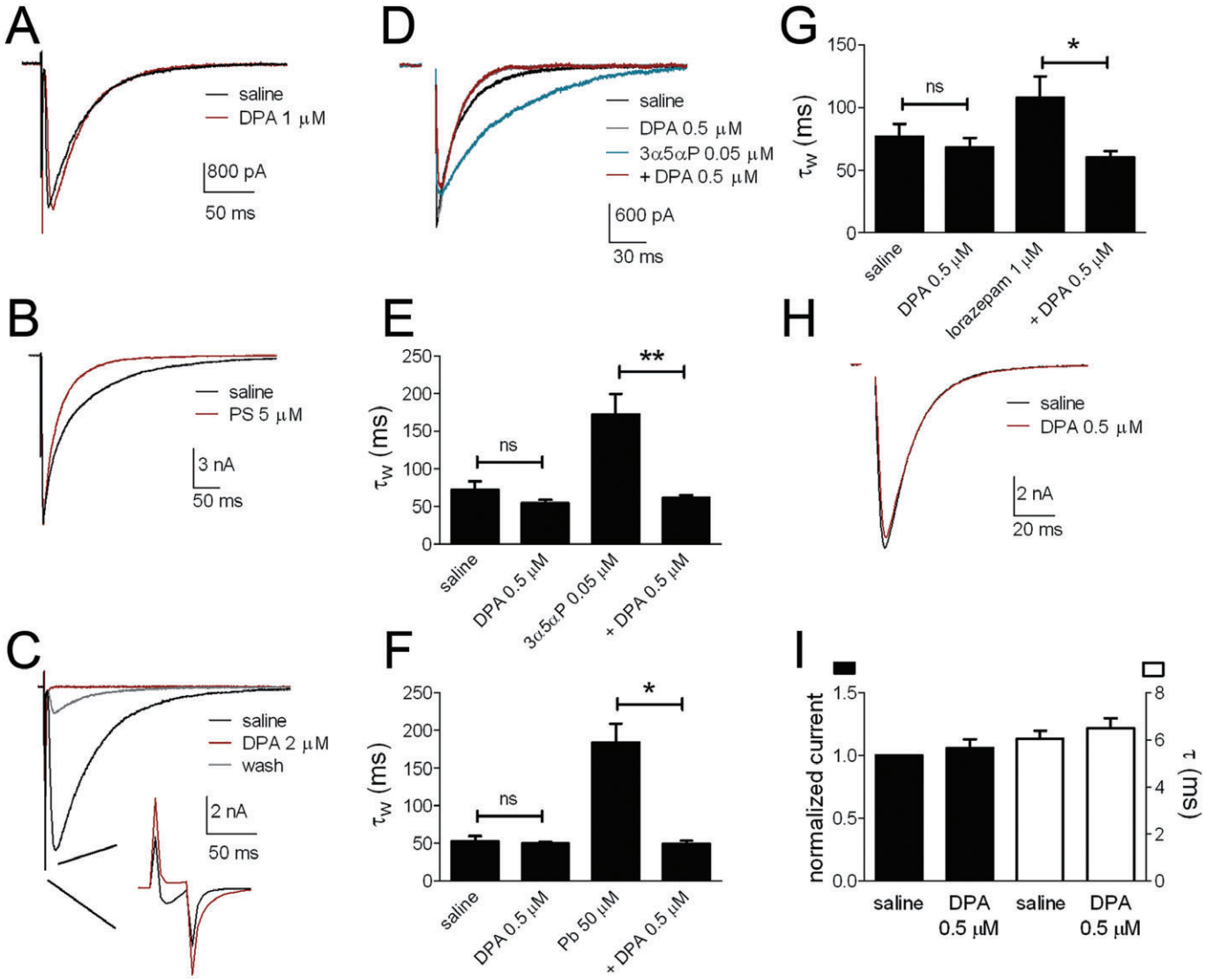

Figure 7

Synaptic effects of DPA. A. Effect of 1 μM DPA on an autaptic IPSC in a hippocampal microculture. DPA caused a slight offset in time of peak IPSC but failed to affect peak amplitude or IPSC decay time. B. For comparison, another IPSC was challenged with 5 μM PS. PS had no effect on the time or amplitude of peak IPSC, but the decay time course was accelerated. See text for summary. C. At 2 μM DPA, IPSCs were eliminated, with a slow partial recovery. Inset: Loss of IPSC was correlated with a large increase in membrane capacitance and near loss of detectable sodium current during stimulation, suggesting a failure of breakaway action potential initiation in the axon. D. Autaptic IPSCs evoked from a hippocampal neuron. The various compounds were pre-applied for 20 s before each sweep. In this cell, there was a small but reliable DPA-induced speeding of the IPSC decay time constant under baseline conditions. However, when the IPSC was prolonged by 3α5αP application, the DPA effect on IPSC decay became much more pronounced. E. Summary of the compounds on weighted IPSC decay time constant (τ_w). $n = 5$ neurons. A two-way, repeated measures ANOVA showed a significant interaction of DPA and potentiator. $^{**}P < 0.01$, ns indicates not significant by Bonferroni corrected *post hoc* *t*-tests. F. Similar pattern of effects when pentobarbital (Pb) was used to prolong IPSCs ($n = 3$ neurons, $^{*}P < 0.05$, ns indicates not significant, two-way ANOVA, *post hoc* *t*-tests). G. The benzodiazepine lorazepam also produced a similar interaction with DPA ($n = 6$ neurons, $^{*}P < 0.05$, ns indicates not significant, two-way ANOVA, *post hoc* *t*-tests). H. Lack of effect of 0.5 μM DPA on a sample EPSC. I. Summary of the effect of 0.5 μM DPA on the peak EPSC and decay time constant from five autaptic glutamatergic neurons.

bicity, negative charge) rather than highly specific structure–activity relationships, we predicted that hydrophobic anions traditionally used as membrane probes would be strong GABA$_A$ receptor antagonists. Two compounds, DPA and TPB, mainstays of classical biophysical studies, indeed strongly antagonize GABA$_A$ receptors. We characterized the more potent of these, DPA, in some detail. Antagonism shared many features with antagonism by sulphated steroids but also exhibited some unexpected properties. Figure 8A–C shows the structures of the compounds found to share mechanistic similarities: DPA, TPB and PS. Structures are presented as stereo pairs to highlight differences amongst the compounds.

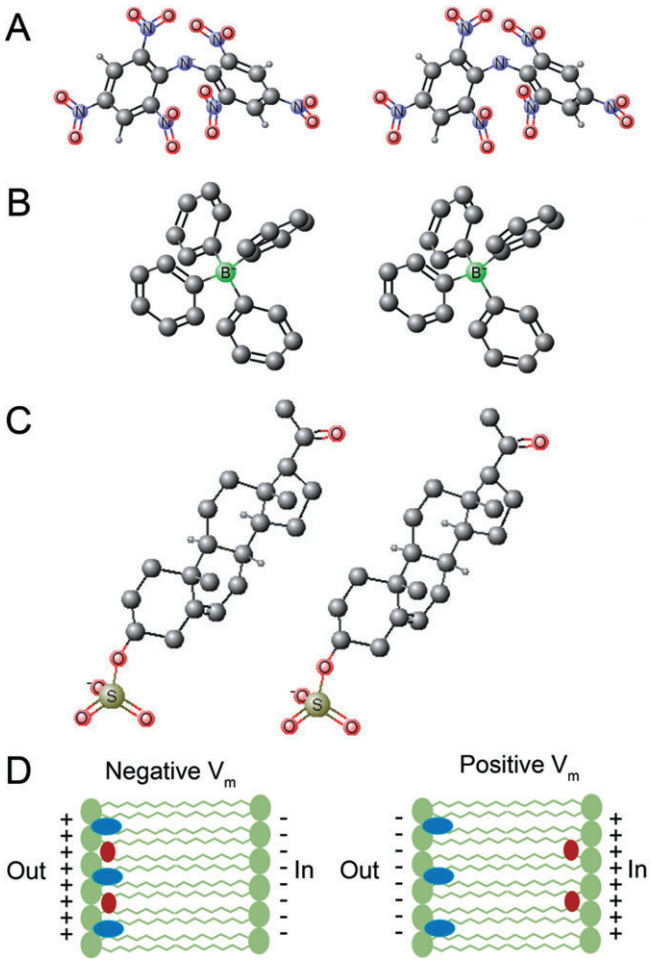

Figure 8

A–C. Stereo pairs of DPA (A), TPB (B), and PS (C). Visual merging of the left and right images highlights three-dimensional structural differences amongst the compounds. D. Diagram of the different behaviour of PS (Mennerick *et al.*, 2008) and DPA (e.g. Bradley *et al.*, 2009) in the membrane at negative (left) and positive (right) membrane potentials.

Judged by aqueous IC_{50} values, DPA is amongst the most potent non-competitive antagonists of $GABA_A$ receptors yet identified. After accounting for the dependence of IC_{50} on GABA concentration, the aqueous IC_{50} concentration for DPA is approximately 10-fold lower than PS and 20-fold lower than picrotoxin (Figure 3A and Eisenman *et al.*, 2003). Aqueous concentrations of DPA that antagonized $GABA_A$ receptors in our studies (e.g. 0.05–0.5 μM) are similar or below those used in studies of membrane excitability and ion channel gating (Bradley *et al.*, 2009). TPB, by contrast, appears to have an IC_{50} similar to PS.

This initial study of DPA did not systematically survey GABA subunit specificity. However, despite heterogeneous cell types in our cultures, including interneurons and principal cells that presumably express a variety of subunit combinations (Fritschy and Mohler, 1995), all cells exhibited strong DPA antagonism. Furthermore, changes in subunit composition during development in culture (Swanwick *et al.*, 2006) did not strongly influence DPA antagonism, as we observed robust DPA antagonism in all cells cultured for 3 to 12 days. A more thorough investigation of possible subunit selectivity awaits further investigation.

Our results suggest that mechanisms of DPA antagonism are similar to those of sulphated neurosteroids. Similarities include a dependence of antagonism on agonist concentration and efficacy, a profile of enhanced apparent desensitization, little steady-state voltage dependence and sensitivity to the α1V256S mutation. This latter point distinguishes the actions of sulphated steroids and DPA from those of picrotoxin (Shen *et al.*, 2000; Akk *et al.*, 2001; Eisenman *et al.*, 2003).

The effect of the α1V256S mutation, at the 2′ position of transmembrane domain 2 (Akk *et al.*, 2001), might suggest that sulphated neurosteroids and DPA bind in the channel. This view is consistent with the recent suggestion of a wide variety of pore-blocking structures for $GABA_A$ receptors (Chen *et al.*, 2006) and with the uncompetitive mechanism of DPA and PS. However, compelling arguments have previously been made that V256 is unlikely to represent part of a binding site for PS. These arguments include the lack of voltage dependence for PS antagonism (expected for a negatively charged ligand binding so deeply within the pore), and the fact that the 2′ mutation in other channel subunits lining the pore do not affect PS antagonism (Akk *et al.*, 2001). A simple channel block is also inconsistent with the peculiar profile of inhibition following removal of aqueous (free) DPA shown in Figure 6A. Particularly at positive potentials, peak GABA responses recover more fully than steady-state responses. This profile is more consistent with modulation of channel gating/desensitization than with channel block. Finally, given our evidence that membrane access is important for DPA antagonism (discussed in detail below), we think it is unlikely that a channel block mechanism by aqueous DPA could explain the uncompetitive antagonism, although we cannot completely exclude this possibility.

DPA also exhibits some points of dissimilarity with PS antagonism. DPA antagonism is more resistant to wash out, especially at positive membrane potentials. Furthermore, IPSCs are more resistant to postsynaptic DPA block than to PS block. Although both compounds induce membrane capacitance increases, DPA-induced capacitive charge movements are voltage-dependent and are much larger, to the point of significantly influencing presynaptic excitability.

Our hypothesis that DPA and TPB are PS-like $GABA_A$ receptor antagonists derived in part from the superficially similar membrane interactions, measured as membrane capacitance increases. Are membrane interactions causally related to $GABA_A$ receptor antagonism? We envision at least three ways that the two phenomena may be linked. First, there may be a specific transmembrane domain on the receptor protein to which the compounds bind, after first partitioning into the membrane. We have proposed a similar model for the positive modulatory actions of 3α-hydroxy neurosteroids at $GABA_A$ receptors (Akk *et al.*, 2005; Chisari *et al.*, 2009; 2010a), and there are several other examples of ligand–receptor binding following obligatory membrane partitioning (Hille, 1977; Lee and MacKinnon, 2004). Although a conventional protein binding site, either transmembrane, pore (see above) or extracellular, is difficult to reconcile with

the wide structural variability amongst antagonist hydrophobic anions (Nilsson *et al.*, 1998; Chisari *et al.*, 2010b), it is possible that each ligand class binds a separate transmembrane domain, with a mechanistically similar outcome.

Another possibility is that that there is no protein binding site on the receptor. Instead, local membrane perturbations induced by the hydrophobic anions may be responsible for the changes in channel gating (Sogaard *et al.*, 2006; Lundbaek, 2008). The latter possibility is difficult to reconcile with the low IC_{50} of DPA, although the IC_{50} may be misleading if the membrane concentration (likely to be much higher than the aqueous concentration) is relevant to receptor interaction. Analyses of related receptor types have suggested structural specificity to sulphated steroid effects, arguing against a direct role for membrane perturbation (Li *et al.*, 2006; Twede *et al.*, 2007). Perhaps additional analysis of the V256S mutation, which appears to uncouple antagonist presence from the alterations in channel gating, could provide additional clues to distinguish amongst the possibilities for a membrane role. At least, the present results indicate that membrane effects of hydrophobic anions participate strongly in the actions of these agents and must be taken into consideration when evaluating antagonism of ion channels.

Whether the hydrophobic anion interaction site(s) represent a proteinaceous or membranous interaction site, the voltage-independence of steady-state DPA antagonism (Figure 5D–F) was puzzling. Because available evidence suggests that PS interacts with the receptor/membrane at an exterior site (Shu *et al.*, 2007; Mennerick *et al.*, 2008) (Figure 8D), we expected that at +40 mV, a potential that drives DPA ions to the inner membrane leaflet (Figure 5C), antagonism would weaken, particularly after removal of extracellular/external DPA. Instead, depolarization dramatically slowed recovery from antagonism (Figure 6A and B). Thus, we favour a model in which DPA antagonizes at an exterior or transmembrane location that is insensitive to membrane potential and that is constantly re-supplied during bath application, but that can also be accessed by DPA from the inner leaflet at positive potentials after removal of aqueous DPA from the bath (Figure 6A and B).

DPA may be an important compound for future studies of negative regulation of $GABA_A$ receptors. The FRET acceptor properties of DPA may be used to probe candidate residues on the $GABA_A$ receptor hypothesized to be important for antagonism. Furthermore, DPA's slow uncompetitive antagonism and irreversibility at positive membrane potentials might prove useful in future studies of $GABA_A$ receptor-mediated transmission, analogous to the utility of use-dependent antagonists of NMDA receptor function (Rosenmund *et al.*, 1993). DPA was relatively inert against $GABA_A$ receptor-mediated autaptic IPSCs in hippocampal neurons. Our results suggest that this is because the elementary lifetime of channel activation resulting from the transient presence of synaptic GABA is too brief for the slow, uncompetitive actions of DPA to be observed. We note, however, that IPSC decay kinetics vary widely across brain regions and synapses (Mody and Pearce, 2004; Capogna and Pearce, 2010). It is possible that differences in subunit composition or transmitter lifetime may promote stronger DPA effects on IPSCs at some synapses, allowing DPA to serve as a probe of the heterogeneity of GABA transmission.

In summary, we have discovered novel $GABA_A$ receptor antagonists that have been mainstays of biophysical studies for decades but whose strong $GABA_A$ receptor antagonist properties have escaped detection. DPA is a particularly potent member of a class of antagonists represented by sulphated neurosteroids and highlights the wide structural variety amongst effective hydrophobic anions. Future studies may exploit the unusual properties of DPA to probe $GABA_A$ receptor structure and function, but when DPA is used for studies of neuronal excitability, its actions on $GABA_A$ receptors should be carefully considered.

Acknowledgements

We thank Larry Eisenman, Joe Henry Steinbach, Gustav Akk and lab members for discussion. We thank John Bracamontes and Joe Henry Steinbach for the α1V256S subunit and Ann Benz and Amanda Taylor for technical help with cultures and oocytes. This work was supported by GM47969 (CFZ) and NS54174 (SM) and the Bantly Foundation. KW was supported by an HHMI SURF fellowship from Washington University.

Conflicts of interest

The authors declare no known conflicts of interest in this work.

References

Akk G, Bracamontes J, Steinbach JH (2001). Pregnenolone sulfate block of $GABA_A$ receptors: mechanism and involvement of a residue in the M2 region of the α subunit. J Physiol (Lond) 532: 673–684.

Akk G, Shu HJ, Wang C, Steinbach JH, Zorumski CF, Covey DF *et al.* (2005). Neurosteroid access to the $GABA_A$ receptor. J Neurosci 25: 11605–11613.

Alexander SP, Mathie A, Peters JA (2009). Guide to Receptors and Channels (GRAC), 4th edition. Br J Pharmacol 158 (Suppl. 1): S1–S254.

Andersen PS, Fuchs M (1975). Potential energy barriers to ion transport within lipid bilayers. Studies with tetraphenylborate. Biophys J 15: 795–830.

Bekkers JM, Stevens CF (1991). Excitatory and inhibitory autaptic currents in isolated hippocampal neurons maintained in cell culture. Proc Natl Acad Sci USA 88: 7834–7838.

Benz R, Läuger P (1977). Transport kinetics of dipicrylamine through lipid bilayer membranes. Effects of membrane structure. Biochim Biophys Acta 468: 245–258.

Benz R, Läuger P, Janko K (1976). Transport kinetics of hydrophobic ions in lipid bilayer membranes. Charge-pulse relaxation studies. Biochim Biophys Acta 455: 701–720.

Bradley J, Luo R, Otis TS, DiGregorio DA (2009). Submillisecond optical reporting of membrane potential in situ using a neuronal tracer dye. J Neurosci 29: 9197–9209.

Bruner LJ (1975). The interaction of hydrophobic ions with lipid bilayer membranes. J Membr Biol 22: 125–141.

Capogna M, Pearce RA (2010). $GABA_{Aslow}$: causes and consequences. Trends Neurosci 34: 101–112.

Chanda B, Asamoah OK, Blunck R, Roux B, Bezanilla F (2005a). Gating charge displacement in voltage-gated ion channels involves limited transmembrane movement. Nature 436: 852–856.

Chanda B, Blunck R, Faria LC, Schweizer FE, Mody I, Bezanilla F (2005b). A hybrid approach to measuring electrical activity in genetically specified neurons. Nat Neurosci 8: 1619–1626.

Chen L, Durkin KA, Casida JE (2006). Structural model for gamma-aminobutyric acid receptor noncompetitive antagonist binding: widely diverse structures fit the same site. Proc Natl Acad Sci USA 103: 5185–5190.

Chisari M, Eisenman LN, Krishnan K, Bandyopadhyaya AK, Wang C, Taylor A *et al*. (2009). The influence of neuroactive steroid lipophilicity on $GABA_A$ receptor modulation: evidence for a low affinity interaction. J Neurophysiol 102: 1254–1264.

Chisari M, Eisenman LN, Covey DF, Mennerick S, Zorumski CF (2010a). The sticky issue of neurosteroids and $GABA_A$ receptors. Trends Neurosci 33: 299–306.

Chisari M, Shu HJ, Taylor A, Steinbach JH, Zorumski CF, Mennerick S (2010b). Structurally diverse amphiphiles exhibit biphasic modulation of $GABA_A$ receptors: similarities and differences with neurosteroid actions. Br J Pharmacol 160: 130–141.

Ebert B, Wafford KA, Whiting PJ, Krogsgaard-Larsen P, Kemp JA (1994). Molecular pharmacology of γ-aminobutyric acid type A receptor agonists and partial agonists in oocytes injected with different α, β, and γ receptor subunit combinations. Mol Pharmacol 46: 957–963.

Eisenman LN, He Y, Fields C, Zorumski CF, Mennerick S (2003). Activation-dependent properties of pregnenolone sulfate inhibition of $GABA_A$ receptor-mediated current. J Physiol (Lond) 550 (Pt 3): 679–691.

Fernandez JM, Taylor RE, Bezanilla F (1983). Induced capacitance in the squid giant axon. Lipophilic ion displacement currents. J Gen Physiol 82: 331–346.

Fritschy JM, Mohler H (1995). $GABA_A$-receptor heterogeneity in the adult rat brain: differential regional and cellular distribution of seven major subunits. J Comp Neurol 359: 154–194.

Hille B (1977). Local anesthetics: hydrophilic and hydrophobic pathways for the drug- receptor reaction. J Gen Physiol 69: 497–515.

Johnson JW, Kotermanski SE (2006). Mechanism of action of memantine. Curr Opin Pharmacol 6: 61–67.

Ketterer B, Neumcke B, Läuger P (1971). Transport mechanism of hydrophobic anions through lipid bilayer membranes. J Membrane Biol 5: 225–245.

Klaassen A, Glykys J, Maguire J, Labarca C, Mody I, Boulter J (2006). Seizures and enhanced cortical GABAergic inhibition in two mouse models of human autosomal dominant nocturnal frontal lobe epilepsy. Proc Natl Acad Sci USA 103: 19152–19157.

Lee SY, MacKinnon R (2004). A membrane-access mechanism of ion channel inhibition by voltage sensor toxins from spider venom. Nature 430: 232–235.

Li W, Covey DF, Alakoskela JM, Kinnunen PK, Steinbach JH (2006). Enantiomers of neuroactive steroids support a specific interaction with the $GABA_C$ receptor as the mechanism of steroid action. Mol Pharmacol 69: 1779–1782.

Lundbaek JA (2008). Lipid bilayer-mediated regulation of ion channel function by amphiphilic drugs. J Gen Physiol 131: 421–429.

Maconochie DJ, Zempel JM, Steinbach JH (1994). How quickly can $GABA_A$ receptors open? Neuron 12: 61–71.

Mennerick S, Que J, Benz A, Zorumski CF (1995). Passive and synaptic properties of neurons grown in microcultures and in mass cultures. J Neurophysiol 73: 320–332.

Mennerick S, Lamberta M, Shu HJ, Hogins J, Wang C, Covey DF *et al*. (2008). Effects on membrane capacitance of steroids with antagonist properties at $GABA_A$ receptors. Biophys J 95: 176–185.

Mody I, Pearce RA (2004). Diversity of inhibitory neurotransmission through $GABA_A$ receptors. Trends Neurosci 27: 569–575.

Nilsson KR, Zorumski CF, Covey DF (1998). Neurosteroid analogues. 6. The synthesis and $GABA_A$ receptor pharmacology of enantiomers of dehydroepiandrosterone sulfate, pregnenolone sulfate, and (3α,5β)-3-hydroxypregnan-20-one sulfate. J Med Chem 41: 2604–2613.

Pennefather P, Quastel DMJ (1992). Modification of dose-response curves by effector blockade and uncompetitive antagonism. Mol Pharmacol 22: 369–380.

Pytel M, Mercik K, Mozrzymas JW (2006). Membrane voltage modulates the $GABA_A$ receptor gating in cultured rat hippocampal neurons. Neuropharmacology 50: 143–153.

Rosenmund C, Clements JD, Westbrook GL (1993). Nonuniform probability of glutamate release at a hippocampal synapse. Science 262: 754–757.

Shen W, Mennerick S, Covey DF, Zorumski CF (2000). Pregnenolone sulfate modulates inhibitory synaptic transmission by enhancing $GABA_A$ receptor desensitization. J Neurosci 20: 3571–3579.

Shu HJ, Eisenman LN, Jinadasa D, Covey DF, Zorumski CF, Mennerick S (2004). Slow actions of neuroactive steroids at $GABA_A$ receptors. J Neurosci 24: 6667–6675.

Shu HJ, Zeng CM, Wang C, Covey DF, Zorumski CF, Mennerick S (2007). Cyclodextrins sequester neuroactive steroids and differentiate mechanisms that rate limit steroid actions. Br J Pharmacol 150: 164–175.

Sogaard R, Werge TM, Bertelsen C, Lundbye C, Madsen KL, Nielsen CH *et al*. (2006). $GABA_A$ receptor function is regulated by lipid bilayer elasticity. Biochemistry 45: 13118–13129.

Swanwick CC, Murthy NR, Mtchedlishvili Z, Sieghart W, Kapur J (2006). Development of gamma-aminobutyric acidergic synapses in cultured hippocampal neurons. J Comp Neurol 495: 497–510.

Twede VD, Covey DF, Tartaglia AL, Bamber BA (2007). The neurosteroids dehydroepiandrosterone sulfate and pregnenolone sulfate inhibit the UNC-49 GABA receptor through a common set of residues. Mol Pharmacol 72: 1322–1329.

Wang M, He Y, Eisenman LN, Fields C, Zeng CM, Mathews J *et al*. (2002). 3β -hydroxypregnane steroids are pregnenolone sulfate-like $GABA_A$ receptor antagonists. J Neurosci 22: 3366–3375.

Weiss DS (1988). Membrane potential modulates the activation of GABA-gated channels. J Neurophysiol 59: 514–527.

Yoon KW, Covey DF, Rothman SM (1993). Multiple mechanisms of picrotoxin block of GABA-induced currents in rat hippocampal neurons. J Physiol (Lond) 464: 423–439.